Journal of Computational and Applied Mathematics 404 (2022) 113410

Contents lists available at ScienceDirect

Journal of Computational and Applied Mathematics

journal homepage: www.elsevier.com/locate/cam

Analysis of a nonlinear singularly perturbed Volterra integro-differential equation

Sumit [a], Sunil Kumar [a,*], Jesus Vigo-Aguiar [b]

[a] Department of Mathematical Sciences, Indian Institute of Technology (BHU) Varanasi, Uttar Pradesh, India
[b] Department of Applied Mathematics, University of Salamanca, Salamanca, Spain

ARTICLE INFO

Article history:
Received 6 December 2020
Received in revised form 5 January 2021

Keywords:
Singularly perturbed
Volterra integro-differential equation
Adaptive mesh generation
Equidistribution principle
A posteriori analysis

ABSTRACT

We consider a nonlinear singularly perturbed Volterra integro-differential equation. The problem is discretized by an implicit finite difference scheme on an arbitrary non-uniform mesh. The scheme comprises of an implicit difference operator for the derivative term and an appropriate quadrature rule for the integral term. We establish both a priori and a posteriori error estimates for the scheme that hold true uniformly in the small perturbation parameter. Numerical experiments are performed and results are reported for validation of the theoretical error estimates.

1. Introduction

Mathematical problems involving small parameter ε with the highest order derivative term are named as singularly perturbed problems. These problems are an important class of problems, because of their regular appearance in many applications in physics, biology, chemistry, and engineering. For small perturbation parameter, the solution of singularly perturbed problems exhibits multiscale character; within some parts of the domain the solution gradient is quite higher than in the other parts. This indicates that to get a convergent numerical solution on uniform meshes, we require the number of mesh points that is inversely proportional to the value of the perturbation parameter, which is computationally not feasible. Therefore, layer adaptive meshes are used to obtain accurate numerical solutions. Broadly there are two classes of such meshes. If a priori information about the location and width of the layers is known, a suitable layer adaptive mesh can be generated a priori (e.g. Shishkin mesh, Bakhvalov mesh, Vulanovic mesh, and so on [1–14]). But, many a times this is not the case. So, it is desirable to generate a suitable layer adaptive mesh a posteriori using some a posterior mesh generation algorithm [15–20].

We consider following singularly perturbed nonlinear Volterra integro-differential equation (VIDE)

$$\begin{cases} \mathcal{T}y := \varepsilon y' + f(x, y(x)) + \displaystyle\int_0^x R(x, s, y(s))\, ds = 0, \quad x \in J = (0, 1], \\ y(0) = B, \end{cases} \tag{1.1}$$

where B is a given constant and $0 < \varepsilon \leq 1$ is a perturbation parameter which in general takes small values. The functions f and R are considered to be sufficiently smooth in $\bar{J} \times \mathbb{R}$ and $\bar{J} \times \bar{J} \times \mathbb{R}$, respectively. Moreover, there exists an $\alpha > 0$ such that $\frac{\partial f}{\partial y} \geq \alpha$ in $\bar{J} \times \mathbb{R}$. Such singularly perturbed VIDEs arise in various physical and biological

* Corresponding author.
E-mail addresses: sumit.rs.mat16@itbhu.ac.in (Sumit), skumar.iitd@gmail.com (S. Kumar), jvigo@usal.es (J. Vigo-Aguiar).

https://doi.org/10.1016/j.cam.2021.113410
0377-0427/

systems, such as diffusion–dissipation processes, filament stretching problems, epidemic dynamics, and synchronous control systems [21–24].

Numerical methods for a linear singularly perturbed VIDE are developed in [19,25–29]. More specifically, an exponential type difference scheme is developed in [26]. In [28] the problem is solved using a fitted operator technique on a piecewise-uniform Shishkin mesh. In [27] a tension spline collocation method is presented. In [25] a backward difference formula is used for the derivative and a repeated quadrature rule is used for the integral term. Further, a Bakhvalov type mesh is used to resolve the layer. In [19] the integrand is considered to be $(x-s)^{-\alpha}y(s)$ with $0<\alpha<1$. Assuming the source term $g(x)$ such that $|g'(x)| \leq (1+x^{-\alpha})$, a posteriori error estimate for a linear VIDE is derived. More precisely, it is proved that $\|\widetilde{Y}-y\|_\infty \leq C \max_{1\leq i\leq N}(h_i^{1-\alpha}+h_i|D^-Y_i|)$, where $\widetilde{Y}$ is the piecewise linear interpolant of the computed solution Y and D^- is the backward difference operator. But surprisingly this a posteriori error estimate is not used for the adaptive mesh generation, instead an arc-length based monitor function is used. Numerical methods for a nonlinear singularly perturbed VIDE are developed in [30,31]. In [30] the nonlinear problem with a special Kernel is solved by asymptotic expansions and an implicit Runge–Kutta method. In [31] a first order uniformly convergent finite difference scheme is constructed on a Bakhvalov type mesh.

To the best of our knowledge, no published paper derived a posteriori error estimate for nonlinear singularly perturbed VIDEs. Further, no published paper on (linear/nonlinear) singularly perturbed VIDEs derived a general criterion that can be used to immediately conclude parameter-uniform convergence of the scheme on a priori constructed layer adapted meshes. These gaps in the literature are the motivation of our work.

We discretize problem (1.1) by an implicit finite difference scheme on an arbitrary non-uniform mesh. The scheme comprises of an implicit difference operator for the derivative term and an appropriate quadrature rule for the integral term. We derive a priori error estimate in the discrete maximum norm based on which we can conclude parameter-uniform convergence of the scheme on a priori meshes, such as Shishkin and Bakhvalov meshes, in the same framework. More importantly, we derive a posteriori error estimate in the maximum norm, which can be used with any adaptive moving mesh procedure. We used a variant of de Boor's algorithm [17,18] for this purpose. Numerical experiments are performed and results are reported for validation of the theoretical error estimates.

The rest of the paper is structured as follows. The next section (Section 2), provides the stability result for the continuous problem (1.1). In Section 3, a finite difference discretization of problem (1.1) is described. A priori and a posteriori error estimates are derived in Sections 4 and 5 , respectively. In Section 6, we provide numerical results for validation of the theoretical error estimates. Finally, some conclusions are given in Section 7.

Notation: We use C as a generic positive constant that does not depend upon ε and the discretization parameter. We simply denote the maximum norm $\sup_{x\in\bar{J}}|g(x)| = \|g\|_\infty$ for any function g on the domain $\bar{J}$. The discrete maximum norm is denoted by $\|.\|_{\bar{\omega}_N}$, $\bar{\omega}_N$ denotes the mesh on $\bar{J}$.

2. Stability of the continuous problem

This section provides the stability result for the continuous problem (1.1). It is used later in a posteriori error analysis of the present numerical scheme for problem (1.1).

Lemma 2.1. *The solution y of (1.1) satisfies the following stability estimate*

$$\|y\|_\infty \leq (|B|+\alpha^{-1}\|F\|_\infty), \quad \text{where} \quad F(x) = -f(x,0) - \int_0^x R(x,s,0)\,ds. \tag{2.1}$$

Further, if y_1 and y_2 are any two functions such that $y_1(0)=y_2(0)$ and

$$\mathcal{T}y_1 - \mathcal{T}y_2 = T,$$

where T is a bounded piecewise continuous function. Then

$$\|y_1-y_2\|_\infty \leq C\|\mathcal{T}y_1-\mathcal{T}y_2\|_\infty. \tag{2.2}$$

Proof. We rewrite problem (1.1) as follows

$$\begin{cases} \widetilde{\mathcal{T}}y := \varepsilon y' + r(x)y(x) + \displaystyle\int_0^x K(x,s)y(s)\,ds = F(x), \quad x\in J=(0,1], \\ y(0)=B, \end{cases} \tag{2.3}$$

where

$$r(x) = \frac{\partial f}{\partial y}(x,\tilde{y}(x)), \quad K(x,s) = \frac{\partial R}{\partial y}(x,s,\hat{y}(s)), \ \tilde{y}(x)=\theta y(x), \ \hat{y}(s)=\gamma y(s), \ 0<\theta,\gamma<1.$$

Now we can use the arguments in [31] to establish (2.1). For proving (2.2), we note that $\mathcal{T}y_1 - \mathcal{T}y_2 = \widetilde{\mathcal{T}}(y_1 - y_2)$, where $\widetilde{\mathcal{T}}$ is defined by (2.3) with

$$r(x) = \frac{\partial f}{\partial y}(x, \bar{y}(x)), \quad K(x,s) = \frac{\partial R}{\partial y}(x, s, \check{y}(s)), \ \bar{y}(x) = y_2(x) + \theta(y_1(x) - y_2(x)),$$

$$\check{y}(s) = y_2(s) + \gamma(y_1(s) - y_2(s)), \ 0 < \theta, \gamma < 1.$$

Thus, (2.2) follows using (2.1). □

3. The discretization and its stability

We consider an arbitrary non-uniform mesh $\omega_N = \{0 < x_1 < \cdots < x_N = 1\}$ to discretize J. We define $\bar{\omega}_N = \{x_0 = 0\} \cup \omega_N$ and $h_i = x_i - x_{i-1}$, $1 \le i \le N$. Further, we define $D^- V_i := \frac{V_i - V_{i-1}}{h_i}$, for any mesh function V. Now integrating (1.1) over (x_{i-1}, x_i), we get

$$h_i^{-1} \int_{x_{i-1}}^{x_i} \mathcal{T}y \, dx = 0. \tag{3.1}$$

Using (1.1) and the right side rectangle formula we get

$$\varepsilon D^- y(x_i) + f(x_i, y(x_i)) + \int_0^{x_i} R(x_i, s, y(s)) \, ds + \mathcal{K}_i^{(1)} + \mathcal{K}_i^{(2)} = 0, \tag{3.2}$$

where

$$\mathcal{K}_i^{(1)} = -h_i^{-1} \int_{x_{i-1}}^{x_i} (\zeta - x_{i-1}) \frac{d}{d\zeta} f(\zeta, y(\zeta)) \, d\zeta$$

and

$$\mathcal{K}_i^{(2)} = -h_i^{-1} \int_{x_{i-1}}^{x_i} (\zeta - x_{i-1}) \frac{d}{d\zeta} \left(\int_0^{\zeta} R(\zeta, s, y(s)) \, ds \right) d\zeta.$$

We next approximate the integral term by the composite left side rectangle formula

$$\int_0^{x_i} R(x_i, s, y(s)) \, ds = \sum_{m=1}^{i} h_m R(x_i, x_{m-1}, y(x_{m-1})) + \mathcal{K}_i^{(3)},$$

where

$$\mathcal{K}_i^{(3)} = \sum_{m=1}^{i} \int_{x_{m-1}}^{x_m} (x_m - \zeta) \frac{d}{d\zeta} R(x_i, \zeta, y(\zeta)) \, d\zeta.$$

On combining the approximations we have the relation

$$\varepsilon D^- y(x_i) + f(x_i, y(x_i)) + \sum_{m=1}^{i} h_m R(x_i, x_{m-1}, y(x_{m-1})) + \mathcal{K}_i = 0, \ i = 1, \ldots, N, \tag{3.3}$$

where

$$\begin{aligned} \mathcal{K}_i &= \mathcal{K}_i^{(1)} + \mathcal{K}_i^{(2)} + \mathcal{K}_i^{(3)} \\ &= -h_i^{-1} \int_{x_{i-1}}^{x_i} (\zeta - x_{i-1}) \frac{d}{d\zeta} f(\zeta, y(\zeta)) \, d\zeta - h_i^{-1} \int_{x_{i-1}}^{x_i} (\zeta - x_{i-1}) \frac{d}{d\zeta} \left(\int_0^{\zeta} R(\zeta, s, y(s)) \, ds \right) d\zeta \\ &\quad + \sum_{m=1}^{i} \int_{x_{m-1}}^{x_m} (x_m - \zeta) \frac{d}{d\zeta} R(x_i, \zeta, y(\zeta)) \, d\zeta. \end{aligned} \tag{3.4}$$

Hence, the discretization of problem (1.1) is proposed as follows

$$\begin{cases} \varepsilon D^- Y_i + f(x_i, Y_i) + \sum_{m=1}^{i} h_m R(x_i, x_{m-1}, Y_{m-1}) = 0, \ i = 1, \ldots, N, \\ Y_0 = B. \end{cases} \tag{3.5}$$

We remark that the authors in [31] used the composite trapezoid rule to approximate the integral term in (3.2). The scheme was proved to be almost first order accurate on Shishkin meshes. Here, we use the composite left side rectangle

formula. One can also consider the composite right side rectangle formula. Here, we present analysis of scheme (3.5). A parallel analysis of the scheme resulting after using the composite right side rectangle formula can also be done.

We next establish that the discrete problem (3.5) is parameter-uniform stable. The following lemma will be used in the proof.

Lemma 3.1. *Consider the discrete problem*

$$\begin{cases} \mathcal{D}^h v_i := \varepsilon D^- v_i + r_i v_i = Q_i, \quad i = 1, \ldots, N, \\ v_0 = B, \end{cases} \tag{3.6}$$

where $r_i \geq \alpha > 0$, $|Q_i| \leq \mathcal{Q}_i$ *with* $\mathcal{Q}_i$ *a non-decreasing function. Then, the solution of* (3.6) *satisfies*

$$|v_i| \leq |B| + \alpha^{-1}\mathcal{Q}_i, \ i = 0, \ldots, N.$$

Proof. It is easy to see that the operator $\mathcal{D}^h$ satisfies the discrete maximum principle. So, considering the mesh function

$$\Psi_i^{\pm} = \pm v_i + |B| + \alpha^{-1}\mathcal{Q}_i,$$

we note that

$$\Psi_0^{\pm} = \pm v_0 + |B| + \alpha^{-1}\mathcal{Q}_0 = \pm B + |B| + \alpha^{-1}\mathcal{Q}_0 \geq 0$$

and

$$\begin{aligned} \mathcal{D}^h \Psi_i^{\pm} &= \pm \mathcal{D}^h v_i + \mathcal{D}^h(|B| + \alpha^{-1}\mathcal{Q}_i) \\ &\geq \pm Q_i + r_i \alpha^{-1}\mathcal{Q}_i \geq \pm Q_i + \mathcal{Q}_i \geq 0, \end{aligned}$$

where we have used $D^-\mathcal{Q}_i \geq 0$ (as $\mathcal{Q}_i$ is a non-decreasing function). Thus, by using the maximum principle for $\mathcal{D}^h$, we get, $\Psi_i^{\pm} \geq 0$, *i.e.*

$$|v_i| \leq |B| + \alpha^{-1}\mathcal{Q}_i, \quad i = 0, \ldots, N. \quad \square$$

Lemma 3.2. *The solution* Y *of the discrete problem* (3.5) *satisfies*

$$\|Y\|_{\bar{\omega}_N} \leq C(|B| + \|\mathcal{F}\|_{\omega_N}), \quad \text{where} \quad \mathcal{F}_i = f(x_i, 0) + \sum_{m=1}^{i} h_m R(x_i, x_{m-1}, 0).$$

Proof. We rewrite the discrete problem (3.5) as follows

$$\varepsilon D^- Y_i + r_i Y_i = Q_i, \quad i = 1, \ldots, N, \quad Y_0 = B$$

with

$$r_i = \frac{\partial f}{\partial y}(x_i, \tilde{Y}_i), \quad Q_i = -\mathcal{F}_i - \sum_{m=1}^{i} h_m \frac{\partial R}{\partial y}(x_i, x_{m-1}, \hat{Y}_{m-1}) Y_{m-1},$$

$$\tilde{Y}_i = \theta Y_i, \ \hat{Y}_m = \gamma Y_m, \ 0 < \theta, \gamma < 1.$$

Now

$$\begin{aligned} |Q_i| &\leq |\mathcal{F}_i| + \sum_{m=1}^{i} h_m \left| \frac{\partial R}{\partial y}(x_i, x_{m-1}, \hat{Y}_{m-1}) \right| |Y_{m-1}| \\ &\leq \|\mathcal{F}\|_{\omega_N} + \sum_{m=1}^{i} h_m \Lambda |Y_{m-1}|, \end{aligned}$$

where $\Lambda = \max |\frac{\partial R}{\partial y}|$. Thus, applying Lemma 3.1, we get

$$|Y_i| \leq |B| + \alpha^{-1}\|\mathcal{F}\|_{\omega_N} + \alpha^{-1} \sum_{m=1}^{i} h_m \Lambda |Y_{m-1}|.$$

So, applying the discrete analogue of Gronwall's inequality [32], we get

$$\|Y\|_{\bar{\omega}_N} \leq (|B| + \alpha^{-1}\|\mathcal{F}\|_{\omega_N}) e^{\alpha^{-1}\Lambda}.$$

Hence, the lemma is proved. $\square$

4. A priori error analysis

The following bound on the derivative of the solution is needed for a priori error analysis, however it is not needed for a posteriori error analysis given in the next section.

Lemma 4.1 ([31]). *The solution y of (1.1) satisfies*

$$|y^{(k)}(x)| \leq C\left(1+\varepsilon^{-k}e^{\frac{-\alpha x}{\varepsilon}}\right),\ x\in\bar{J},\ k=0,1. \tag{4.1}$$

Lemma 4.2. *For the solutions y and Y of (1.1) and (3.5), respectively, we have*

$$\|Y-y\|_{\bar{\omega}_N} \leq C \max_{1\leq i\leq N}|\mathcal{K}_i|.$$

Proof. Using (3.3) and (3.5), and the arguments in Lemma 3.2 the proof easily follows. □

Theorem 4.1. *Suppose y is the solution of (1.1) and Y is the solution of (3.5). Then*

$$\|Y-y\|_{\bar{\omega}_N} \leq C\vartheta(\omega_N),$$

where $\vartheta(\omega_N)=\max_{1\leq i\leq N}\int_{x_{i-1}}^{x_i}(1+\varepsilon^{-1}e^{\frac{-\alpha\zeta}{\varepsilon}})d\zeta$.

Proof. We shall find bounds of the components of the error term $\mathcal{K}_i$ one by one. We proceed as follows

$$\begin{aligned}
|\mathcal{K}_i^{(1)}| &\leq h_i^{-1}\int_{x_{i-1}}^{x_i}|(\zeta-x_{i-1})|\left|\frac{d}{d\zeta}f(\zeta,y(\zeta))\right|d\zeta\\
&= h_i^{-1}\int_{x_{i-1}}^{x_i}|(\zeta-x_{i-1})|\left|\frac{\partial f}{\partial\zeta}(\zeta,y(\zeta))+y'(\zeta)\frac{\partial f}{\partial y}(\zeta,y(\zeta))\right|d\zeta\\
&\leq C\int_{x_{i-1}}^{x_i}(1+|y'(\zeta)|)\,d\zeta,
\end{aligned} \tag{4.2}$$

$$\begin{aligned}
|\mathcal{K}_i^{(2)}| &\leq h_i^{-1}\int_{x_{i-1}}^{x_i}|(\zeta-x_{i-1})|\left|\frac{d}{d\zeta}\left(\int_0^{\zeta}R(\zeta,s,y(s))\,ds\right)\right|d\zeta\\
&= h_i^{-1}\int_{x_{i-1}}^{x_i}|(\zeta-x_{i-1})|\left|R(\zeta,\zeta,y(\zeta))+\int_0^{\zeta}\frac{\partial R}{\partial\zeta}(\zeta,s,y(s))\,ds\right|d\zeta\\
&\leq C\int_{x_{i-1}}^{x_i}d\zeta,
\end{aligned} \tag{4.3}$$

$$\begin{aligned}
|\mathcal{K}_i^{(3)}| &\leq \sum_{m=1}^{i}\int_{x_{m-1}}^{x_m}|(x_m-\zeta)|\left|\frac{dR}{d\zeta}(x_i,\zeta,y(\zeta))\right|d\zeta\\
&= \sum_{m=1}^{i}\int_{x_{m-1}}^{x_m}|(x_m-\zeta)|\left|\frac{\partial R}{\partial\zeta}(x_i,\zeta,y(\zeta))+y'(\zeta)\frac{\partial R}{\partial y}(x_i,\zeta,y(\zeta))\right|d\zeta\\
&\leq C\sum_{m=1}^{i}h_m\int_{x_{m-1}}^{x_m}(1+|y'(\zeta)|)\,d\zeta\\
&\leq C\left(\max_{1\leq m\leq i}\int_{x_{m-1}}^{x_m}(1+|y'(\zeta)|)\,d\zeta\right)\left(\sum_{m=1}^{i}h_m\right)\\
&\leq C\max_{1\leq m\leq i}\int_{x_{m-1}}^{x_m}(1+|y'(\zeta)|)\,d\zeta.
\end{aligned} \tag{4.4}$$

Thus, on combining the bounds of these three components from (4.2), (4.3) and (4.4), we get

$$|\mathcal{K}_i| \leq C\max_{1\leq m\leq i}\int_{x_{m-1}}^{x_m}(1+|y'(\zeta)|)\,d\zeta.$$

Hence, using (4.1) and Lemma 4.2, the proof is completed. □

We can apply Theorem 4.1 to a number of a priori defined layer adapted meshes. Below we consider standard Shishkin and Bakhvalov meshes.

4.1. Shishkin meshes

Shishkin meshes are defined with the help of a transition parameter σ_s defined by

$$\sigma_s = \min\left\{0.5, \frac{\varepsilon}{\alpha}\ln N\right\}. \tag{4.5}$$

Now $[0, 1]$ is divided into two sub-intervals $[0, \sigma_s]$ and $[\sigma_s, 1]$ by the transition parameter σ_s, which again are divided into $N/2$ uniform subintervals. Note that these meshes are piecewise uniform in nature. On this mesh, we have $\vartheta(\omega_N) \leq C(N^{-1}\ln N)$, cf. [33]. Hence, by Theorem 4.1, we get

$$\|Y - y\|_{\overline{\omega}_N} \leq C(N^{-1}\ln N).$$

4.2. Bakhvalov meshes

Bakhvalov meshes give more accuracy than Shishkin meshes. There are several ways to construct these meshes. Our construction is based on the equidistribution of the function

$$\varphi(\zeta) := \max\left\{1, \frac{\kappa}{\varepsilon}e^{-\alpha\zeta/\varepsilon}\right\}$$

with a user chosen positive constant κ; that is, the mesh points x_i are so that

$$\int_0^{x_i}\varphi(\zeta)d\zeta = \frac{i}{N}\int_0^1\varphi(\zeta)d\zeta.$$

Bakhvalov meshes are graded in nature. On this mesh, we have $\vartheta(\omega_N) \leq CN^{-1}$, cf. [33]. Hence, by Theorem 4.1, we get

$$\|Y - y\|_{\overline{\omega}_N} \leq CN^{-1}.$$

5. A posteriori error analysis

We now provide a posteriori error analysis for the discrete problem (3.5). Suppose $\widetilde{Y}$ is the piecewise linear interpolant of the numerical solution $\{Y_i\}$, so that $\widetilde{Y}$ is continuous on J, linear on each $[x_{i-1}, x_i]$, and $\widetilde{Y}(x_i) = Y_i$, $0 \leq i \leq N$. Further, for $x \in (x_{i-1}, x_i)$, we have

$$\widetilde{Y}(x) = Y_i + (x - x_i)D^-Y_i \quad \text{and} \quad \widetilde{Y}(x) = Y_{i-1} + (x - x_{i-1})D^-Y_i.$$

Theorem 5.1. *Suppose y is the solution of (1.1), Y is the solution of (3.5) on an arbitrary mesh $\{x_i\}$, and $\widetilde{Y}$ is its piecewise linear interpolant. Then*

$$\|\widetilde{Y} - y\|_\infty \leq C\max_{1\leq i\leq N} h_i\left\{1 + |D^-Y_i| + h_i|D^-Y_i|^2\right\}.$$

Proof. Using (1.1) we get

$$\mathcal{T}\widetilde{Y}(x) - \mathcal{T}y(x) = \varepsilon(\widetilde{Y}(x))' + f(x, \widetilde{Y}(x)) + \int_0^x R(x, s, \widetilde{Y}(s))ds.$$

Note that $(\widetilde{Y}(x))' = D^-Y_i$, $x \in (x_{i-1}, x_i)$, $1 \leq i \leq N$. We define auxiliary functions p and q by $p(x) := f(x, \widetilde{Y}(x))$ and $q(x, s) := R(x, s, \widetilde{Y}(s))$, respectively. Suppose $\widetilde{p}$ is the piecewise linear interpolant of p on $\overline{\omega}_N$. Further, suppose $\widetilde{q}$ is the piecewise linear interpolant of q in s variable on $\overline{\omega}_N$. Note that $p(x_i) = f(x_i, Y_i)$ and $q(x_i, x_{m-1}) = R(x_i, x_{m-1}, Y_{m-1})$. Also, for $x \in (x_{i-1}, x_i)$ and $s \in (x_{m-1}, x_m)$, we have

$$\widetilde{p}(x) = p(x_i) + (x - x_i)D^-p(x_i) \quad \text{and} \quad \widetilde{q}(x, s) = q(x, x_{m-1}) + (s - x_{m-1})D^-q(x, x_m).$$

Using these auxiliary functions and their interpolants, for $x \in (x_{i-1}, x_i)$, we have

$$\begin{aligned}
\mathcal{T}\widetilde{Y}(x) - \mathcal{T}y(x) &= \varepsilon(\widetilde{Y}(x))' + p(x) + \int_0^x q(x, s)\,ds \\
&= \varepsilon(\widetilde{Y}(x))' + \widetilde{p}(x) + (p(x) - \widetilde{p}(x)) + \int_0^x \left(\widetilde{q}(x, s) + \left(q(x, s) - \widetilde{q}(x, s)\right)\right) ds \\
&= \varepsilon D^-Y_i + \left(p(x_i) + (x - x_i)D^-p(x_i)\right) + \left(p(x) - \widetilde{p}(x)\right)
\end{aligned}$$

$$
\begin{aligned}
&+ \sum_{m=1}^{i-1} \int_{x_{m-1}}^{x_m} \left[q(x, x_{m-1}) + (s - x_{m-1}) D^- q(x, x_m)\right] ds \\
&+ \int_{x_{i-1}}^{x} \left[q(x, x_{i-1}) + (s - x_{i-1}) D^- q(x, x_i)\right] ds + \int_0^x (q(x, s) - \widetilde{q}(x, s)) \, ds \\
&+ \sum_{m=1}^{i} h_m q(x_i, x_{m-1}) - \sum_{m=1}^{i} h_m q(x_i, x_{m-1}) \\
&= (x - x_i) D^- p(x_i) + \left(p(x) - \widetilde{p}(x)\right) + \sum_{m=1}^{i} h_m \left(q(x, x_{m-1}) - q(x_i, x_{m-1})\right) \\
&+ \sum_{m=1}^{i-1} \int_{x_{m-1}}^{x_m} (s - x_{m-1}) D^- q(x, x_m) \, ds + \int_{x_{i-1}}^{x} (s - x_{i-1}) D^- q(x, x_i) \, ds \\
&+ \int_0^x (q(x, s) - \widetilde{q}(x, s)) \, ds + (x - x_{i-1}) q(x, x_{i-1}). \qquad (5.1)
\end{aligned}
$$

Now we estimate separately each of the terms in (5.1). Using the standard interpolation error estimate, for $x \in (x_{i-1}, x_i)$, we have

$$
|p(x) - \widetilde{p}(x)| \le \left\{ \frac{h_i^2}{8} \sup_{(x_{i-1}, x_i)} |p''(x)| \right\},
$$

where

$$
p''(x) = f_{xx}(x, \widetilde{Y}(x)) + 2(\widetilde{Y}(x))' f_{xy}(x, \widetilde{Y}(x)) + [(\widetilde{Y}(x))']^2 f_{yy}(x, \widetilde{Y}(x)).
$$

Therefore, for $x \in (x_{i-1}, x_i)$, we have

$$
|p(x) - \widetilde{p}(x)| \le C h_i^2 \left(1 + |D^- Y_i| + |D^- Y_i|^2\right). \qquad (5.2)
$$

Similarly, for $x \in (x_{i-1}, x_i)$ and $s \in (x_{m-1}, x_m)$, $m = 1, 2 \ldots, i$, we have

$$
|q(x, s) - \widetilde{q}(x, s)| \le C h_m^2 \left(1 + |D^- Y_m| + |D^- Y_m|^2\right).
$$

Consequently,

$$
\begin{aligned}
\left| \int_0^x (q(x, s) - \widetilde{q}(x, s)) \, ds \right| &\le \sum_{m=1}^{i-1} \int_{x_{m-1}}^{x_m} |q(x, s) - \widetilde{q}(x, s)| \, ds + \int_{x_{i-1}}^{x} |q(x, s) - \widetilde{q}(x, s)| \, ds \\
&\le C \max_{1 \le m \le i} \left\{ h_m^2 \left(1 + |D^- Y_m| + |D^- Y_m|^2\right) \right\} \left(\sum_{m=1}^{i-1} \int_{x_{m-1}}^{x_m} ds + \int_{x_{i-1}}^{x} ds \right) \\
&\le C \max_{1 \le m \le i} \left\{ h_m^2 \left(1 + |D^- Y_m| + |D^- Y_m|^2\right) \right\}. \qquad (5.3)
\end{aligned}
$$

Also,

$$
\begin{aligned}
|D^- p(x_i)| &= \left| \frac{f(x_i, \widetilde{Y}(x_i)) - f(x_{i-1}, \widetilde{Y}(x_{i-1}))}{h_i} \right| \\
&= \left| \frac{f(x_i, \widetilde{Y}(x_i)) - f(x_{i-1}, \widetilde{Y}(x_i)) + f(x_{i-1}, \widetilde{Y}(x_i)) - f(x_{i-1}, \widetilde{Y}(x_{i-1}))}{h_i} \right| \\
&\le \left| \frac{\partial f}{\partial x}(\xi_i^{(1)}, \widetilde{Y}(x_i)) \right| + \left| \frac{\partial f}{\partial y}(x_{i-1}, \sigma_i^{(1)}) \right| |D^- Y_i|, \qquad (5.4)
\end{aligned}
$$

where $\xi_i^{(1)} \in (x_{i-1}, x_i)$ and $\sigma_i^{(1)} \in (\widetilde{Y}(x_{i-1}), \widetilde{Y}(x_i))$. Thus, we get

$$
|D^- p(x_i)| \le C(1 + |D^- Y_i|). \qquad (5.5)
$$

Using similar calculations we get

$$
|D^- q(x, x_m)| \le \left| \frac{\partial R}{\partial s}(x, \xi_m^{(2)}, \widetilde{Y}(x_m)) \right| + \left| \frac{\partial R}{\partial y}(x, x_m, \sigma_m^{(2)}) \right| |D^- Y_m|,
$$

where $\xi_m^{(2)} \in (x_{m-1}, x_m)$ and $\sigma_m^{(2)} \in (\widetilde{Y}(x_{m-1}), \widetilde{Y}(x_m))$. Thus, we get

$$|D^- q(x, x_m)| \le C(1 + |D^- Y_m|). \tag{5.6}$$

Now

$$\begin{aligned}
&\left|\sum_{m=1}^{i-1}\int_{x_{m-1}}^{x_m}(s - x_{m-1})D^- q(x, x_m)\,ds\right| + \left|\int_{x_{i-1}}^{x}(s - x_{i-1})D^- q(x, x_i)\,ds\right| \\
&\le \sum_{m=1}^{i-1} h_m|D^- q(x, x_m)|\int_{x_{m-1}}^{x_m} ds + h_i|D^- q(x, x_i)|\int_{x_{i-1}}^{x} ds \\
&\le \max_{1\le m\le i} h_m|D^- q(x, x_m)|\left(\sum_{m=1}^{i-1}\int_{x_{m-1}}^{x_m} ds + \int_{x_{i-1}}^{x} ds\right) \\
&\le C \max_{1\le m\le i} h_m(1 + |D^- Y_m|),
\end{aligned} \tag{5.7}$$

$$\sum_{m=1}^{i} h_m\left|q(x, x_{m-1}) - q(x_i, x_{m-1})\right| \le Ch_i \quad \text{and} \quad |(x - x_{i-1})q(x, x_{i-1})| \le Ch_i. \tag{5.8}$$

Now using all these estimates from (5.2)–(5.8) in (5.1), we obtain

$$\|\mathcal{T}\widetilde{Y} - \mathcal{T}y\|_\infty \le C \max_{1\le i\le N} h_i\left\{1 + |D^- Y_i| + h_i|D^- Y_i|^2\right\}. \tag{5.9}$$

Hence, from Lemma 2.1, we get the desired a posteriori error estimate. □

6. Numerical experiments

We consider the following test problem

$$\begin{cases} \varepsilon y' + y^3 + 3y + \int_0^x y^2(s)\,ds = e^{-\frac{3x}{\varepsilon}} - \frac{1}{2}\varepsilon e^{-\frac{2x}{\varepsilon}} + 2e^{-\frac{x}{\varepsilon}} + \frac{\varepsilon}{2}, \quad x \in (0, 1], \\ y(0) = 1. \end{cases} \tag{6.1}$$

The exact solution of the test problem is given by $y(x) = e^{-\frac{x}{\varepsilon}}$. The quasilinearization technique for nonlinear problems is a Newton like method which gives an iterative scheme [31,34] for the discrete problem (3.5) as follows

$$\begin{cases} Y_i^{(r)} = \dfrac{P_i Y_{i-1}^{(r)} - f(x_i, Y_i^{(r-1)}) - \frac{\partial f}{\partial y}(x_i, Y_i^{(r-1)})Y_i^{(r-1)} - A_i}{P_i + \frac{\partial f}{\partial y}(x_i, Y_i^{(r-1)})}, \quad i = 1, \ldots, N, \\ Y_0^{(r)} = B, \end{cases} \tag{6.2}$$

where $Y_i^{(0)}$ is given and

$$\begin{aligned} P_i &= \varepsilon/h_i, \\ A_i &= \sum_{k=1}^{i} h_k R(x_i, x_{k-1}, Y_{k-1}^{(r)}). \end{aligned} \tag{6.3}$$

We use the condition

$$\max_i \left|Y_i^{(r)} - Y_i^{(r-1)}\right| \le 10^{-5},$$

as the stopping criterion, and $Y_i^{(0)} = 0$ as the initial iteration for the iterative scheme.

We consider adaptive mesh generation algorithm originally proposed by de Boor [35]. In literature, it has been utilized for several classes of singularly perturbed problems (see [17–20,36,37] and the references therein). The convergence of the algorithm is studied in [38] for singularly perturbed problems and in [39] for regular boundary value problems. Starting with a uniform mesh the algorithm constructs a mesh that solves the equidistribution problem

$$h_i\psi_i = \frac{1}{N}\sum_{j=1}^{N}\psi_j h_j, \quad 1 \le i \le N, \tag{6.4}$$

where the monitor function ψ is chosen from the a posteriori error estimate. For our problem, $\psi_i = 1 + |D^- Y_i| + h_i|D^- Y_i|^2$, as suggested by Theorem 5.1. It was pointed out in [38] that it is not necessary to enforce (6.4) strictly. It is sufficient to

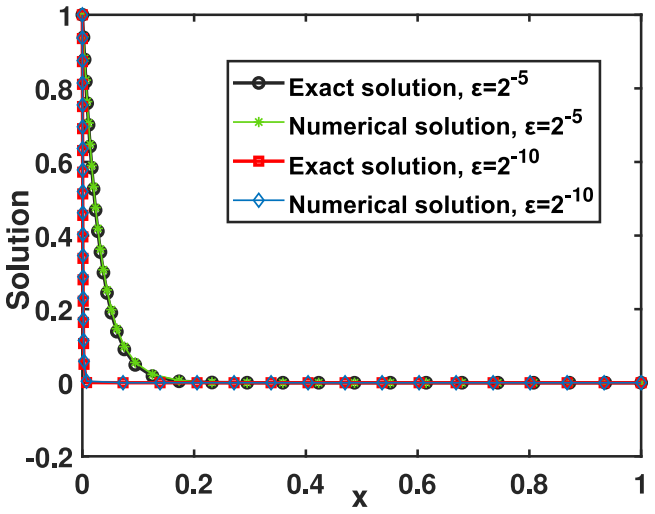

Fig. 1. The exact and numerical solutions obtained using scheme (3.5) on a posteriori meshes with $N = 64$.

stop the algorithm when the following weakened equidistribution principle

$$h_i\psi_i \le \frac{C_0}{N}\sum_{j=1}^{N}\psi_j h_j, \quad 1 \le i \le N, \tag{6.5}$$

is satisfied for some constant $C_0 > 1$.

Algorithm.
Input: $N \in \mathbb{N}$, $0 < \varepsilon \le 1$ and $C_0 = 1.1$.
Output: Equidistributed mesh $\{x_i\}$ and the solution Y_i.

Step 1. Define the initial iteration of the adaptive mesh ($k = 0$) as a uniform mesh $x_i^{(0)} = i/N$, $i = 0, \ldots, N$.
Step 2. Calculate $Y_i^{(k)}$ solving the discrete problem (3.5) on the mesh $\{x_i^{(k)}\}$.
Step 3. Set $h_i^{(k)} = x_i^{(k)} - x_{i-1}^{(k)}$ and evaluate the discretized monitor function $\psi_i^{(k)}$, for $i = 1, \ldots, N$. Compute $\Psi_i^{(k)} = \sum_{j=1}^{i} h_j^{(k)}\psi_j^{(k)}$.
Step 4. Check for the stopping criterion; if $\max_{1\le i\le N} h_i^{(k)}\psi_i^{(k)} \le C_0\frac{\Psi_N^{(k)}}{N}$ holds, go to Step 6, else continue with next step.
Step 5. Set $Z_i = i\frac{\Psi_N}{N}$ for $i = 0, \ldots, N$. Generate a new mesh $\{x_i^{(k+1)}\}$ by interpolating the points (Ψ_i^k, x_i^k) and evaluating this interpolant at Z_i, $i = 0, 1, \ldots, N$. Return to step 2 setting $k = k + 1$.
Step 6. Take $\{x_i^{(k)}\}$ as the final adaptive mesh and $Y_i^{(k)}$ as the adaptive solution. Stop.

Now we shall apply the proposed method on the test problem (6.1) and discuss the numerical observations in the form of tables and figures. The numerical solution obtained on the a posteriori mesh is compared with the exact solution for two different values of ε in Fig. 1, which also confirms the presence of a boundary layer near $x = 0$. We compute the solutions for the set $E_\varepsilon = \{10^{-1}, 10^{-2}, \ldots, 10^{-7}\}$ of values of ε and using different values of the discretization parameter N. The maximum pointwise errors and corresponding rates of convergence are calculated by

$$F_\varepsilon^N = \max_{1\le i\le N}\left|Y_i^{\varepsilon,N} - y_i^{\varepsilon}\right|, \qquad \varrho_\varepsilon^N = \log_2\left(F_\varepsilon^N/F_\varepsilon^{2N}\right).$$

The parameter-uniform errors and parameter-uniform rates of convergence are computed as follows

$$F^N = \max_{\varepsilon}\{F_\varepsilon^N\}, \qquad \varrho^N = \log_2\left(F^N/F^{2N}\right).$$

These errors and rates of convergence obtained on a priori and a posteriori generated adaptive meshes are organized in the tabular form. In Table 1, the results are given on a posteriori generated meshes. Tables 2 and 3 show the results on Shishkin and Bakhvalov meshes, respectively. The experimentally obtained errors and convergence rates in Table 1 clearly confirm the optimal first order parameter-uniform convergence of scheme (3.5) on the a posteriori generated mesh. Table 4 provides a comparison of the parameter-uniform errors and parameter-uniform convergence rates for various meshes. Table 5 lists the maximum pointwise errors, rates of convergence, and the number of iterations required by the algorithm for different values of C_0 (in the stopping criterion). In addition, log–log graphs of the maximum pointwise

Table 1
Errors F_ε^N and F^N, and convergence rates ϱ_ε^N and ϱ^N using a posteriori error estimate of Theorem 5.1.

$\varepsilon = 10^{-r}$	$N = 32$	$N = 64$	$N = 128$	$N = 256$	$N = 512$	$N = 1024$	$N = 2048$
$r = 1$	7.6288e−03	3.8598e−03	1.9535e−03	9.8294e−04	4.9301e−04	2.4689e−04	1.2354e−04
	0.9886	0.9825	0.9909	0.9955	0.9977	0.9989	
$r = 2$	8.8662e−03	4.6227e−03	2.3514e−03	1.1873e−03	5.8714e−04	2.9690e−04	1.4924e−04
	0.9396	0.9752	0.9858	1.0159	0.9837	0.9923	
$r = 3$	9.1101e−03	4.7863e−03	2.4622e−03	1.2483e−03	6.3252e−04	3.1732e−04	1.5908e−04
	0.9285	.9590	0.9800	0.9808	0.9952	0.9962	
$r = 4$	9.1352e−03	4.5723e−03	2.4789e−03	1.2625e−03	6.3824e−04	3.2124e−04	1.6124e−04
	0.9985	0.8832	0.9734	0.9841	0.9905	0.9944	
$r = 5$	9.1385e−03	4.8102e−03	2.3495e−03	1.2637e−03	6.3907e−04	3.2177e−04	1.6157e−04
	0.9926	1.0338	0.8947	0.9836	0.9899	0.9939	
$r = 6$	9.1381e−03	4.8110e−03	2.4804e−03	1.1964e−03	6.3916e−04	3.2182e−04	1.6161e−04
	0.9256	0.9558	1.0518	0.9045	0.9899	0.9938	
$r = 7$	9.1502e−03	4.8109e−03	2.4892e−03	1.2638e−03	6.3919e−04	3.2183e−04	1.6161e−04
	.9275	0.9506	0.9779	0.9835	0.9899	0.9938	
F^N	9.1502e−03	4.8109e−03	2.4892e−03	1.2638e−03	6.3919e−04	3.2183e−04	1.6161e−04
ϱ^N	.9275	.9506	.9779	.9835	.9899	.9938	

Table 2
Errors F_ε^N and F^N, and convergence rates ϱ_ε^N and ϱ^N using a priori generated Shishkin mesh.

$\varepsilon = 10^{-r}$	$N = 32$	$N = 64$	$N = 128$	$N = 256$	$N = 512$	$N = 1024$	$N = 2048$
$r = 1$	1.5734e−02	9.6739e−03	5.7331e−03	2.9809e−03	1.4979e−03	7.5086e−04	3.7591e−04
	0.7017	0.7548	0.9435	0.9928	0.9964	0.9982	
$r = 2$	1.4715e−02	9.0424e−03	5.3571e−03	3.0921e−03	1.7502e−03	9.7587e−04	5.3785e−04
	0.7025	0.7553	0.7929	0.8210	0.8428	0.8595	
$r = 3$	1.4612e−02	8.9788e−03	5.3219e−03	3.0717e−03	1.7391e−03	9.6988e−04	5.3457e−04
	0.7026	0.7546	0.7929	0.8207	0.8425	0.8594	
$r = 4$	1.4602e−02	8.9724e−03	5.3183e−03	3.0697e−03	1.7380e−03	9.6928e−04	5.3424e−04
	0.7026	0.7545	0.7929	0.8206	0.8425	0.8594	
$r = 5$	1.4601e−02	8.9718e−03	5.3180e−03	3.0694e−03	1.7379e−03	9.6922e−04	5.3421e−04
	0.7026	0.7545	0.7929	0.8206	0.8425	0.8594	
$r = 6$	1.4601e−02	8.9717e−03	5.3179e−03	3.0694e−03	1.7379e−03	9.6921e−04	5.3421e−04
	0.7026	0.7545	0.7929	0.8206	0.8425	0.8594	
$r = 7$	1.4601e−02	8.9717e−03	5.3179e−03	3.0694e−03	1.7379e−03	9.6921e−04	5.3421e−04
	0.7026	0.7545	0.7929	0.8206	0.8425	0.8594	
F^N	1.4601e−02	8.9717e−03	5.3179e−03	3.0694e−03	1.7379e−03	9.6921e−04	5.3421e−04
ϱ^N	0.7026	0.7545	0.7929	0.8206	0.8425	0.8594	

Table 3
Errors F_ε^N and F^N, and convergence rates ϱ_ε^N and ϱ^N using a priori generated Bakhvalov mesh.

$\varepsilon = 10^{-r}$	$N = 32$	$N = 64$	$N = 128$	$N = 256$	$N = 512$	$N = 1024$	$N = 2048$
$r = 1$	9.6826e−03	5.0027e−03	2.5462e−03	1.2850e−03	6.4553e−04	3.2354e−04	1.6196e−04
	0.9527	0.9744	0.9866	0.9932	0.9966	0.9983	
$r = 2$	9.4011e−03	4.8938e−03	2.5095e−03	1.2743e−03	6.4341e−04	3.2372e−04	1.6250e−04
	0.9419	0.9636	0.9777	0.9859	0.9910	0.9943	
$r = 3$	9.3859e−03	4.8786e−03	2.4987e−03	1.2689e−03	6.4064e−04	3.2229e−04	1.6177e−04
	0.9440	0.9653	0.9775	0.9860	0.9912	0.9944	
$r = 4$	9.3838e−03	4.8770e−03	2.4973e−03	1.2684e−03	6.4035e−04	3.2214e−04	1.6170e−04
	0.9442	0.9656	0.9774	0.9861	0.9912	0.9944	
$r = 5$	9.3836e−03	4.8768e−03	2.4972e−03	1.2683e−03	6.4032e−04	3.2213e−04	1.6169e−04
	0.9442	0.9656	0.9774	0.9861	0.9912	0.9944	
$r = 6$	9.3836e−03	4.8768e−03	2.4972e−03	1.2683e−03	6.4031e−04	3.2213e−04	1.6169e−04
	0.9442	0.9656	0.9774	0.9861	0.9912	0.9944	
$r = 7$	9.3836e−03	4.8768e−03	2.4972e−03	1.2683e−03	6.4031e−04	3.2213e−04	1.6169e−04
	0.9442	0.9656	0.9774	0.9861	0.9912	0.9944	
F^N	9.3836e−03	4.8768e−03	2.4972e−03	1.2683e−03	6.4031e−04	3.2213e−04	1.6169e−04
ϱ^N	0.9442	0.9656	0.9774	0.9861	0.9912	0.9944	

errors are plotted in Fig. 2 for each mesh with two different values of ε. The slopes of these plots match the slopes of the theoretical order plots, which again authenticates our theoretical findings. One can observe that the errors are larger for Shishkin meshes than on Bakhvalov and a posteriori meshes, as seen with the theory as well. Further, the errors are similar on Bakhvalov meshes and a posteriori generated meshes. However, the construction of Bakhvalov meshes requires a priori information about the location and width of the layers. Whereas, for a posteriori meshes no a priori information is required for the solution.

Table 4
Parameter-uniform errors F^N and parameter-uniform convergence rates ϱ^N using scheme (3.5) on various meshes.

Mesh		$N = 64$	$N = 128$	$N = 256$	$N = 512$	$N = 1024$	$N = 2048$
A posteriori mesh	F^N	4.8109e−03	2.4892e−03	1.2638e−03	6.3919e−04	3.2183e−04	1.6161e−04
	ϱ^N	0.9506	0.9779	0.9835	0.9899	0.9938	
Shishkin mesh	F^N	8.9717e−03	5.3179e−03	3.0694e−03	1.7379e−03	9.6921e−04	5.3421e−04
	ϱ^N	0.7545	0.7929	0.8206	0.8425	0.8594	
Bakhvalov mesh	F^N	4.8768e−03	2.4972e−03	1.2683e−03	6.4031e−04	3.2213e−04	1.6169e−04
	ϱ^N	0.9656	0.9774	0.9861	0.9912	0.9944	

Table 5
Maximum errors F_ε^N, convergence rates ϱ_ε^N, and the number of iterations k taking $\varepsilon = 2^{-10}$ and using different values of C_0 in the algorithm.

C_0		$N = 64$	$N = 128$	$N = 256$	$N = 512$	$N = 1024$	$N = 2048$
$C_0 = 1.15$	F_ε^N	4.6827e−03	2.4396e−03	1.2467e−03	6.3188e−04	3.1696e−04	1.5153e−04
	ϱ_ε^N	0.9407	0.9685	0.9804	0.9954	1.0647	
	k	3	3	3	3	3	2
$C_0 = 1.5$	F_ε^N	4.6827e−03	2.4396e−03	1.3907e−03	5.6301e−04	2.8688e−04	1.5153e−04
	ϱ_ε^N	0.9407	0.8109	1.3046	0.9727	0.9208	
	k	3	3	2	2	2	2
$C_0 = 2.0$	F_ε^N	4.6827e−03	3.4833e−03	1.3907e−03	5.6301e−04	2.8688e−04	1.5153e−04
	ϱ_ε^N	0.4269	1.3247	1.3046	0.9727	0.9208	
	k	3	2	2	2	2	2
$C_0 = 3.0$	F_ε^N	8.5563e−03	3.4833e−03	1.3907e−03	5.6301e−04	2.8688e−04	1.5153e−04
	ϱ_ε^N	1.2965	1.3247	1.3046	0.9727	0.9208	
	k	2	2	2	2	2	2

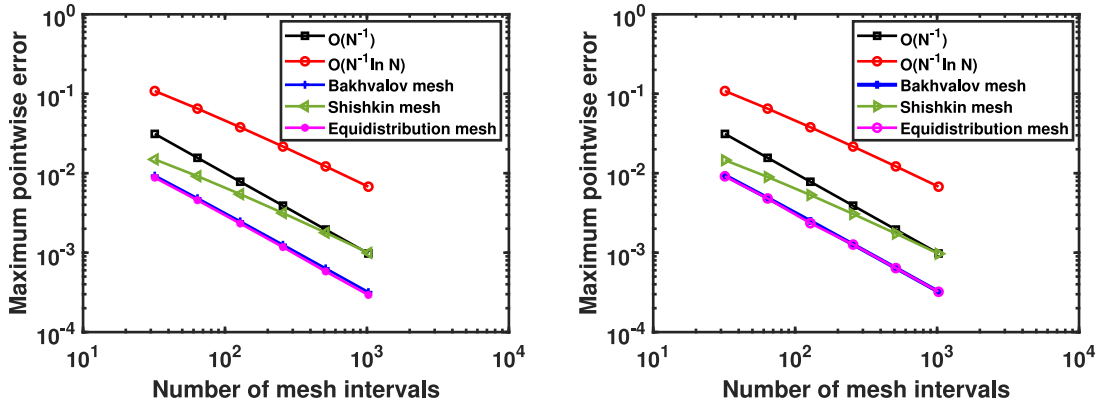

(a) For $\varepsilon = 10^{-2}$ (b) For $\varepsilon = 10^{-5}$

Fig. 2. Log–log plots of error vs N for $\varepsilon = 10^{-2}$ and $\varepsilon = 10^{-5}$.

To show the adaptive nature of the a posteriori generated mesh, in Fig. 3, we have given the mesh trajectory as the algorithm moves with the iterations and the final a posteriori mesh points position. The mesh points are condensing towards the left boundary and finally adapt the solution behaviour by itself. This confirms the adaptivity of the a posteriori generated mesh.

7. Conclusions

A nonlinear singularly perturbed VIDE is considered. The discretization of the problem is done on an arbitrary non-uniform mesh by an implicit finite difference scheme which comprises of an implicit difference operator for the derivative term and an appropriate quadrature rule for the integral term. We have derived a priori error estimate in the discrete maximum norm based on which the scheme is proved to be uniformly convergent on Shishkin and Bakhvalov meshes in the same framework. After that a posteriori error estimate in the maximum norm is established for the scheme that holds true uniformly in ε. Numerical experiments are performed and results are reported for validation of the theoretical error estimates.

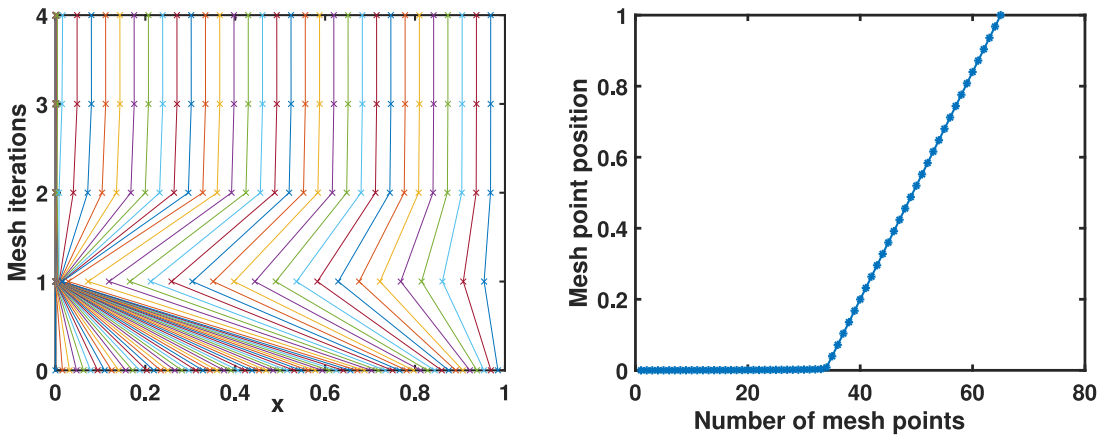

(a) Mesh trajectory (b) Mesh points position

Fig. 3. Movement of mesh points through few iterations and the final adaptive mesh position for $N = 64$ and $\varepsilon = 2^{-10}$.

Acknowledgements

This research was supported by the Science and Engineering Research Board (SERB), India under the Project No. ECR/2017/000564. The first author gratefully acknowledges the support of University Grants Commission, India, for research fellowship with Reference No: 20/12/2015(ii)EU-V. The authors gratefully acknowledge the valuable comments and suggestions from the anonymous referees.

References

[1] N.S. Bakhvalov, On the optimization of the methods for solving boundary value problems in the presence of a boundary layer, Zh. Vychisl. Mat. Mat. Fiz. 9 (4) (1969) 841–859.
[2] R. Vulanović, Non-equidistant generalizations of the gushchin-shchennikov scheme, ZAMM-J. Appl. Math. Mech./Z. Angew. Math. Mech. 67 (12) (1987) 625–632.
[3] R. Vulanović, A priori meshes for singularly perturbed quasilinear two-point boundary value problems, IMA J. Numer. Anal. 21 (1) (2001) 349–366.
[4] H.-G. Roos, M. Stynes, L. Tobiska, Robust Numerical Methods for Singularly Perturbed Differential Equations: Convection–Diffusion-Reaction and Flow Problems, Vol. 24, Springer Science & Business Media, 2008.
[5] J.J.H. Miller, E. O'Riordan, G.I. Shishkin, Fitted Numerical Methods for Singular Perturbation Problems, World Scientific Co., Singapore, 1996.
[6] C. Clavero, J. Vigo-Aguiar, Numerical approximation of 2D time dependent singularly perturbed convection–diffusion problems with attractive or repulsive turning points, Appl. Math. Comput. 317 (2018) 223–233.
[7] H. Ramos, J. Vigo-Aguiar, S. Natesan, R.G. Rubio, M.A. Queiruga, Numerical solution of nonlinear singularly perturbed problems on nonuniform meshes by using a non-standard algorithm, J. Math. Chem. 48 (2010) 38–54.
[8] S. Natesan, J. Jayakumar, J. Vigo-Aguiar, Parameter uniform numerical method for singularly perturbed turning point problems exhibiting boundary layers, J. Comput. Appl. Math. 158 (1) (2003) 121–134.
[9] K. Kumar, P.P. Chakravarthy, J. Vigo-Aguiar, Numerical solution of time-fractional singularly perturbed convection–diffusion problems with a delay in time, Math. Methods Appl. Sci. (2020) http://dx.doi.org/10.1002/mma.6477.
[10] S. Kumar, Layer-adapted methods for quasilinear singularly perturbed delay differential problems, Appl. Math. Comput. 233 (2014) 214–221.
[11] S. Kumar, M. Kumar, A second order uniformly convergent numerical scheme for parameterized singularly perturbed delay differential problems, Numer. Algorithms 76 (2) (2017) 349–360.
[12] S. Kumar, M. Kumar, Analysis of some numerical methods on layer adapted meshes for singularly perturbed quasilinear systems, Numer. Algorithms 71 (1) (2016) 139–150.
[13] S. Kumar, M. Kumar, Parameter-robust numerical method for a system of singularly perturbed initial value problems, Numer. Algorithms 59 (2) (2012) 185–195.
[14] S.C.S. Rao, S. Kumar, Second order global uniformly convergent numerical method for a coupled system of singularly perturbed initial value problems, Appl. Math. Comput. 219 (8) (2012) 3740–3753.
[15] P. Das, J. Vigo-Aguiar, Parameter uniform optimal order numerical approximation of a class of singularly perturbed system of reaction diffusion problems involving a small perturbation parameter, J. Comput. Appl. Math. 354 (2019) 533–544.
[16] D. Shakti, J. Mohapatra, P. Das, J. Vigo-Aguiar, A moving mesh refinement based optimal accurate uniformly convergent computational method for a parabolic system of boundary layer originated reaction–diffusion problems with arbitrary small diffusion terms, J. Comput. Appl. Math. (2020) 113167.
[17] N. Kopteva, M. Stynes, A robust adaptive method for a quasi-linear one-dimensional convection–diffusion problem, SIAM J. Numer. Anal. 39 (2001) 1446–1467.
[18] P. Das, Comparison of a priori and a posteriori meshes for singularly perturbed nonlinear parameterized problems, J. Comput. Appl. Math. 290 (2015) 16–25.
[19] J. Huang, Z. Cen, A. Xu, L.-B. Liu, A posteriori error estimation for a singularly perturbed Volterra integro-differential equation, Numer. Algorithms 83 (2) (2020) 549–563.

[20] S. Kumar, S. Kumar, Sumit, High-order convergent methods for singularly perturbed quasilinear problems with integral boundary conditions, Math. Methods Appl. Sci. (2020) http://dx.doi.org/10.1002/mma.6854.
[21] J.S. Angell, W.E. Olmstead, Singularly perturbed Volterra integral equations II, SIAM J. Appl. Math. 47 (6) (1987) 1150–1162.
[22] F. Hoppensteadt, An algorithm for approximate solutions to weakly filtered synchronous control systems and nonlinear renewal processes, SIAM J. Appl. Math. 43 (4) (1983) 834–843.
[23] A.S. Lodge, J.B. McLeod, J.A. Nohel, A nonlinear singularly perturbed Volterra integrodifferential equation occurring in polymer rheology, Proc. R. Soc. Edinburgh Sect. A 80 (1–2) (1978) 99–137.
[24] G.S. Jordan, A nonlinear singularly perturbed Volterra integrodifferential equation of nonconvolution type, Proc. R. Soc. Edinburgh Sect. A 80 (3–4) (1978) 235–247.
[25] B.C. Iragi, J.B. Munyakazi, A uniformly convergent numerical method for a singularly perturbed Volterra integro-differential equation, Int. J. Comput. Math. 97 (4) (2020) 759–771.
[26] A. Salama, D.J. Evans, Fourth order scheme of exponential type for singularly perturbed Volterra integro-differential equations, Int. J. Comput. Math. 77 (1) (2001) 153–164.
[27] V. Horvat, M. Rogina, Tension spline collocation methods for singularly perturbed Volterra integro-differential and Volterra integral equations, J. Comput. Appl. Math. 140 (1–2) (2002) 381–402.
[28] Ö. Yapman, G.M. Amiraliyev, A novel second-order fitted computational method for a singularly perturbed Volterra integro-differential equation, Int. J. Comput. Math. (2019) 1–10.
[29] Y. Liang, L. Liu, Z. Cen, A posteriori error estimation in maximum norm for a system of singularly perturbed Volterra integro-differential equations, Comput. Appl. Math. (2020) http://dx.doi.org/10.1007/s40314-020-01303-7.
[30] J.-P. Kauthen, Implicit Runge-Kutta methods for some integrodifferential–algebraic equations, Appl. Numer. Math. 13 (1–3) (1993) 125–134.
[31] S. Şevgin, Numerical solution of a singularly perturbed Volterra integro-differential equation, Adv. Difference Equ. 2014 (1) (2014) 171.
[32] D. Willett, J. Wong, On the discrete analogues of some generalizations of gronwall's inequality, Monatsh. Math. 69 (4) (1965) 362–367.
[33] T. Linß, Layer-Adapted Meshes for Reaction-Convection–Diffusion Problems, Springer, 2009.
[34] U.M. Ascher, R.M. Mattheij, R.D. Russell, Numerical Solution of Boundary Value Problems for Ordinary Differential Equations, Vol. 13, SIAM, 1994.
[35] C. de Boor, Good approximation by splines with variable knots, in: Spline Functions and Approximation Theory, Proceedings of the symposium held at the University of Alberta, Birkhauser, Edmonton, Basel, 1973.
[36] S. Kumar, Sumit, H. Ramos, Parameter-uniform approximation on equidistributed meshes for singularly perturbed parabolic reaction–diffusion problems with robin boundary conditions, Appl. Math. Comput. 392 (2021) 125677.
[37] S. Kumar, Sumit, J. Vigo-Aguiar, A parameter-uniform grid equidistribution method for singularly perturbed degenerate parabolic convection–diffusion problems, J. Comput. Appl. Math. (2020) 113273.
[38] N. Kopteva, M. Stynes, A robust adaptive method for a quasi-linear one-dimensional convection–diffusion problem, SIAM J. Numer. Anal. 39 (4) (2001) 1446–1467.
[39] X. Xu, W. Huang, R.D. Russell, J.F. Williams, Convergence of de Boor's algorithm for the generation of equidistributing meshes, IMA J. Numer. Anal. 31 (2) (2010) 580–596.